ISSN 1392–1320 MATERIALS SCIENCE (MEDŽIAGOTYRA). Vol. XX, No. X. 2023

Microstructure and Properties of 6 Series Aluminum Alloy Under Different Aging Treatment Systems

Qi YIN [1]*, Liping JIANG [1], Fengjia GUO [2], Zhaoxia WANG [2]

[1] *College of Engineering, Yantai Nanshan University, Yantai 265713, China*
[2] *Shandong Nanshan Aluminum Co., Ltd., Yantai 265713, China*

http://dx.doi.org/10.5755/j02.ms.32988

Received 15 December 2022; accepted 14 March 2023

In the present study, an investigation is conducted into the effect of different aging treatments on the hardening properties of the 6151 aluminum alloy sheet. According to the research results, the artificial aging hardening response of the pre-aging sheet is significantly stronger compared to natural aging after the solution treatment. In the stage of artificial aging, 120 °C pre-aging treatment produces a more significant strengthening effect than 80 °C and 100 °C pre-aging treatment. The longer the artificial time, the higher the hardness value. When the artificial aging temperature reaches 200 °C, the time taken to achieve peak aging is the shortest, and the occurrence of softening is evident in the over-aged state. When the artificial aging temperature is 200 °C, the softening effect becomes more significant. Natural aging can inhibit the strengthening effect of artificial aging. With the extension of natural aging, the hardening effect of artificial aging diminishes gradually.
Keywords: aluminum alloy, aging, microstructure, mechanical properties.

1. INTRODUCTION

6xxx series aluminum alloy demonstrates various advantages such as excellent formability and mechanical properties, strong corrosion resistance and ease of processing, which makes it widely applicable in the automobile industry [1]. It has the advantages of high strength and excellent corrosion resistance, and can be applied to automobile body structural parts and some external covering parts [2, 3]. Automobile lightweight is the inevitable trend of automobile production. At present, the aluminum alloys widely used in the automobile industry include 2 xxx series [4], 5xxx series and 6xxx series, for the production of automobile inner and outer plates. Some well-known automobile manufacturers such as Audi and Ford have succeeded in the development of all-aluminum body [5].

6xxx series aluminum alloy performs well in heat treatment. By coating and baking the formed plate, high hardness and yield strength can be achieved after age hardening, while the plate obtained after solution treatment stagnates at room temperature for some time. The hardening that occurs in the course of natural aging tends to hinder the strengthening effect of artificial aging (simulated paint baking) [6, 7]. The typical aging precipitation sequence of 6-series aluminum alloy is: supersaturated solid solution (SSSS)→solute atom segregation zone (G.P.) →β"→β′→β(Mg_2Si). Since there are other alloying elements in the alloy, when the ratio of different alloying elements changes, the precipitated phase of the alloy will change [8].

According to some research, pre-aging treatment can suppress hardening in the natural aging process, which leads to relatively low T4 yield strength and improves the artificial aging hardening response effectively [9, 10]. The atomic clusters or GP regions of thr aluminum alloy after pre-aging are larger than those of natural aging. Therefore, it can serve as the nucleating core of the β" phase- the main strengthening phase. The precipitation of phase can significantly improve the baking hardening ability of the plate.

6151 aluminum alloy is a deformed aluminum alloy developed in the United States, with good corrosion resistance and forging performance. Its strength is slightly higher than 6061. 6151 aluminum alloy is suitable for manufacturing medium-strength complex forgings and supercharger impellers for machinery and automobile parts. With the 6151 aluminum alloy plate in different states as the research object, this study aims to find the best solution to improving the response of artificial age hardening by revealing the effect of aging treatment on artificial age hardening in different processes.

2. MATERIALS AND METHODS

The material used for the experiment is a 6151 aluminum alloy cold-rolled sheet, the composition of which is shown in Table 1. With a thickness of 1.6mm, the sheet of the experimental specimen was cut into multiple test pieces sized 12 × 17 mm.

Table 1. Composition of 6151 aluminum alloy

Element	Al	Mg	Si	Cu	Fe	Mn	Cr	Ti
Content, wt%	Bal	1.0	0.8	0.4	0.18	0.29	0.08	0.06

The experimental specimen was treated with a solid solution at 550 °C for 5 min, then quenched in water immediately after the solid solution. After water quenching, aging treatment was performed in different ways, as shown in Fig. 1. Firstly, after the pre-aging treatment carried out at 80 °C, 100 °C and 120 °C, it stopped at room

*Correspondingauthor. Tel.: +535-8590701.
E-mail address: *jianglina@nanshan.com.cn* (Q. Yin)

temperature, and then artificial aging occurred. The aging temperature was set to 160 ºC, 180 ºC and 200 ºC, while the holding time was set to 20 min, 30 min and 40 min. Secondly, the test pieces obtained after solution treatment were treated for different periods of time: 0 h, 1 h, 2 h, 4 h, 6 h, 8 h, 10 h, 24 h, 48 h, 60 h and 72 h, while the artificial aging temperature was set to 160 ºC, 180 ºC and 200 ºC. The effect of artificial aging time on strengthening properties was analyzed. Lastly, artificial aging treatment was carried out on the specimens given different durations of natural aging from 0 to 14 days, an aging temperature of 200 ºC and a holding time of 2 h. The effect of natural aging on artificial aging hardening was analyzed.

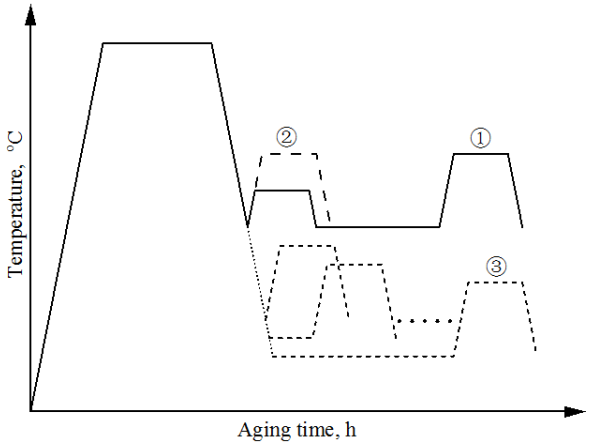

Fig. 1. Diagram of the aging process

The hardness of samples as obtained after different aging treatments was measured by using a MH-5l microhardness tester. The load was set to 500 g and the loading time was set to 20 s. Material's crystallographic structure was determined by X-ray diffraction (XRD) measurement with a D/Max 2500V/PC diffractometer (Rigaku Corporation, Japan) and Cu K<alpha> targets (λ = 0.154 nm), at a scanning rate of 0.0202θ s^{-1}.The transmission specimens were prepared under different aging conditions by means of ion thinning (PIPS) (voltage 6 kV, room temperature), and the transmission experiment was carried out by using JEOL JEM-2100F transmission instrument to examine the microstructure.

3. EXPERIMENTAL RESULTS AND DISCUSSION

3.1. Effect of pre-aging treatment on the artificial aging hardening of 6151 sheet

Fig. 2 shows the effect of the artificial aging process on the strengthening properties of materials under different aging conditions. It can be seen from the figure that the hardness of materials in different pre-aging states shows an upward trend with the extension of artificial aging time and the rise of aging temperature. The artificial aging hardening response of the pre-aged specimen is significantly stronger compared to the naturally aged specimen. Besides, given the same aging temperature, artificial aging hardness increases with the rise of the pre-aging temperature. This is because there are more atomic clusters and GP regions in the aluminum matrix with the increase of the pre-aging temperature, which provides more nucleation points for the formation of the second phase.

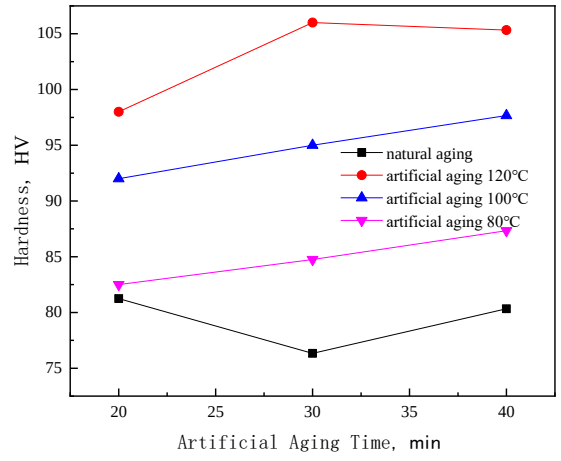

a

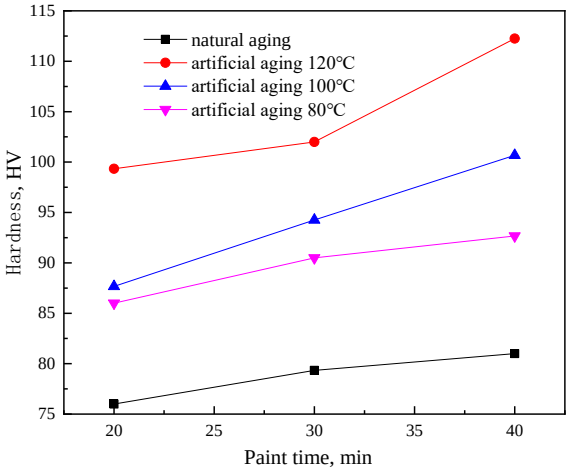

b

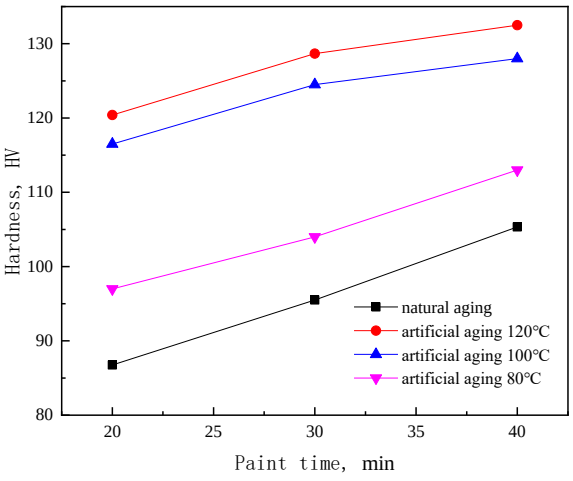

c

Fig. 2. Effect of pre-aging treatment on artificial aging hardening at different artificial aging temperature: a – aging temperature 160 ºC; b – aging temperature 180 ºC; c – aging temperature 200 ºC

The more and finer the strengthening phase that develops during artificial aging, the higher the hardness

value of the material [11]. The higher the artificial aging temperature, the more significant the strengthening property, and the more it precipitates in the process of artificial aging β". The longer the artificial aging time, the more extensive and uniform the phase is, and the better the strengthening effect.

As for the specimens in the natural aging state, the hardness of the material increases with the extension of the artificial aging time at the artificial aging temperature of 180 °C and 200 °C. However, when the aging temperature reaches 160 °C, the hardness of the material decreases first and then increases with the extension of the aging time. This is because the GP zone formed in the natural aging process is re-dissolved during the artificial aging process, which decreases the strengthening effect of the GP zone on the matrix [12]. According to the study of Lorimer et al. [13] on the precipitation nucleation kinetics, only the GP region in excess of a certain critical size has the potential to develop into the core of transition phase precipitation. However, the size of the GP region formed in natural aging is very small, which is adverse to the occurrence of nucleation. In the course of artificial aging, these GP zones are re-dissolved into the aluminum matrix to precipitate again, which explains why the artificial aging response of the naturally aged specimen is less significant than that of the pre-aged specimen.

By comparing the hardness of specimens as obtained in different aging states after artificial aging, it can be found out that the parameters of an aging process that produces the best artificial aging hardening effect for 6151 aluminum alloy are as follows: a pre-aging temperature of 120 °C, an artificial aging temperature of 200 °C and a holding time of 40 min. In this case, the hardness reaches 134 HV after artificial aging.

3.2. Effect of artificial aging time on strengthening performance of 6151 sheet

Fig. 3 shows the curve of changes in hardness value with aging time for 6151 aluminum alloy plate at different artificial aging temperatures of 160 °C, 180 °C and 200 °C. It can be seen from the figure that when the artificial aging temperature varies, the hardness curve of the specimen changes in the same way. With the extension of artificial aging time, the hardness value decreases gradually after reaching a certain peak, but the response rate of artificial aging hardening differs. The time taken for the specimen to reach the maximum hardness at the artificial aging temperature of 160 °C, 180 °C and 200 °C is 4 h, 10 h and 24 h, respectively. With the rise of artificial aging temperature, there is a sharp increase in the hardening rate of the specimen. There are two reasons for this. On the one hand, the increase of atomic kinetic energy is accompanied by a sharp rise in the precipitation and growth rate of the second phase. On the other hand, the response rate of artificial aging improves with the rise of the artificial aging temperature. As shown in Fig. 3, the aging hardening curve at an artificial aging temperature of 200 °C shows a more significant aging softening effect that at 160 °C and 180 °C. Its hardness value drops steeply to 105 HV after reaching the peak value of 125 HV, and then it decreases at a slow pace. This is possibly attributed to a large amount of metastable state β". The phase expands rapidly at high temperatures and shifts into a relatively stable β′ phase, because it is partially coherent with the matrix β′. Since the strengthening effect of the relative matrix is less significant than that of the coherent matrix β" phase, there is a rapid reduction in the hardness of the specimen.

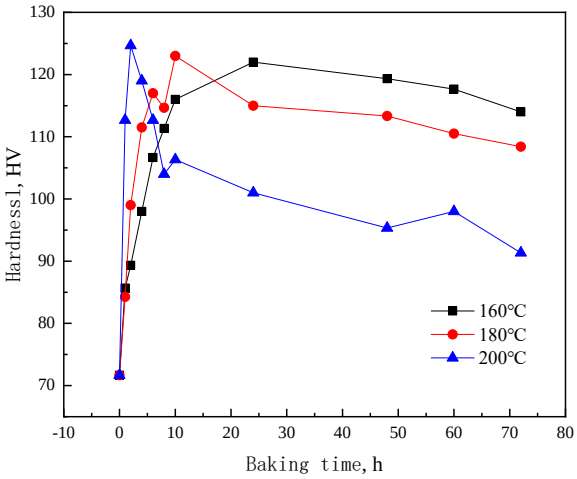

Fig. 3. The change of hardness value with the aging time at different artificial aging temperature

Fig. 4 shows the TEM structure as observed at different stages at the artificial aging temperature of 200 °C. Fig. 4 a presents the microstructure of solid solution state, showing no obvious precipitated structure in the aluminum matrix. As shown in Fig. 4 b, there are plenty of uniformly distributed point precipitates in the matrix. Since the precipitate is extremely small, it is difficult to determine its crystal structure. However, its spherical shape is found highly consistent with that of the GP region of the 6-series alloy. In addition to the GP region, there is a tiny fraction of needle-like precipitation in the matrix β" phase, despite its smaller size.

Fig. 4 c shows the TEM image of the specimen captured after 4 h of artificial aging at 200 °C. It can be seen from the figure that there are a large number of circular precipitates formed in the alloy and distributed along three $<100>_{Al}$ directions. According to some research, these precipitates are of the β" phase. Most of the granular precipitates shown in Fig. 4 c are β". This is the cross-section of the phase, and the rest represents the undissolved GP area. They are small and evenly distributed β". The phase significantly increases the difficulty in free movement of dislocations and thus the strength of the alloy [14]. Phase β" is considered to be the main strengthening phase in 6-series aluminum alloy.

Fig. 4 d shows the TEM image in the overaged state. Unlike in the peak aged state, the spherical GP region disappears and the needle-like β" emerges. Increasingly replaced by a large number of rod-shaped precipitates, the phase is usually referred to as β′ phase. Due to the re-dissolution of GP area, the formation of rod β′ phase and the growth of phase β", the hardness value of the alloy declines gradually. Besides, the longer the holding time, the less extensive the phase β", the more the rod precipitates and the lower the hardness value.

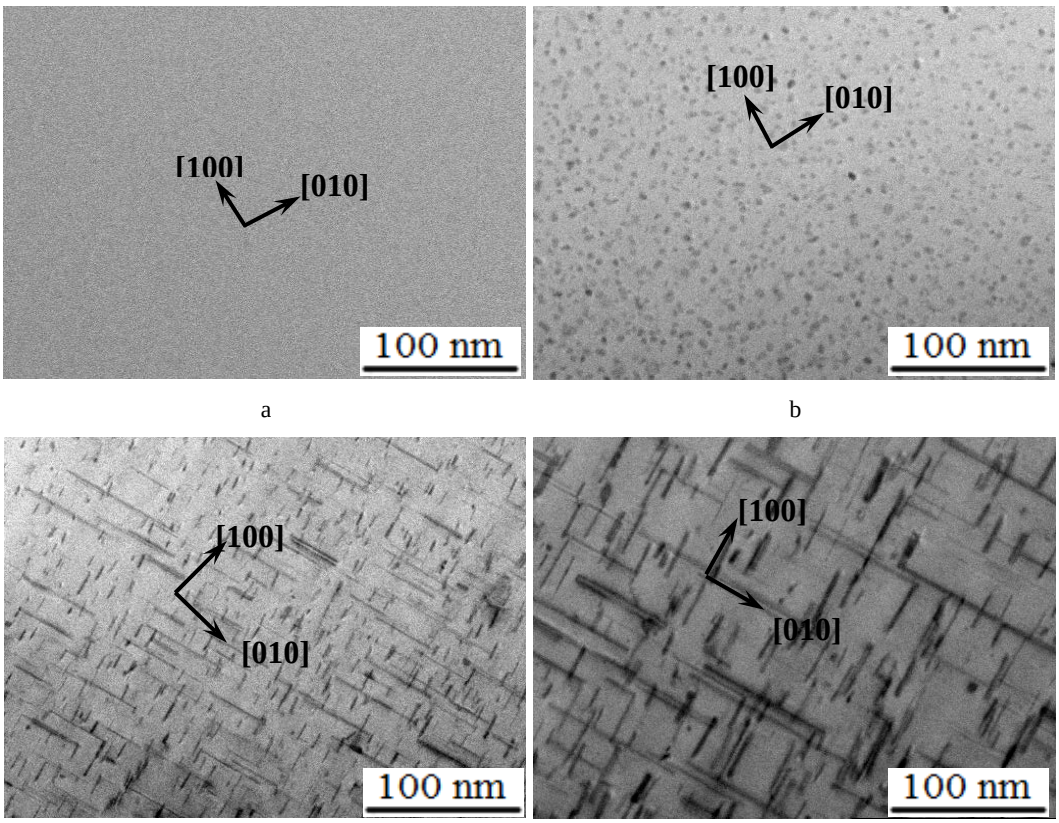

Fig. 4. TEM images of different states of artificial aging temperature 200 °C: a – not-aged; b – under-aged; c – peak-aged; d – over-aged

Fig. 5 shows the XRD patterns of 6151 aluminum alloy in different states at the artificial aging temperature of 200 °C. As is shown in the figure, there are the diffraction peaks of Mg_2Si, Mg_2Cu and AlMnSi in addition to the diffraction peaks of aluminum alloy a-Al matrix under artificial aging.

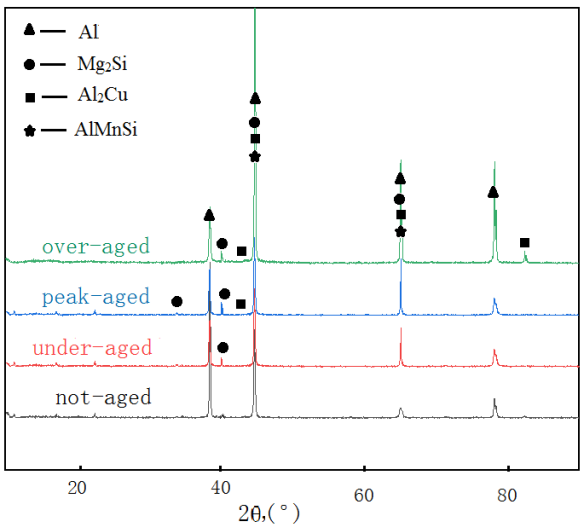

Fig. 5. XRD results of the 6151 aluminum alloys after 200 °C artificial aging

When the alloy is in the initial test state, there are basically no other obvious diffraction peaks except for the relatively high diffraction peaks of the a-Al matrix; The diffraction peak of Mg_2Si is wide and short during under-aging, which means that Mg_2Si phase begins to precipitate fine and is in microcrystalline state and GP region appears at this time; When the sample is in the peak aging state, it can be seen that the diffraction peak intensity has obvious changes, the Mg_2Si diffraction peak increases, and the Mg_2Si diffraction peak further increases in the over-aging state, and the second phase begins to form. This corresponds to TEM images of different states of artificial aging temperature 200 °C in Fig. 4.

3.3. Effect of natural aging on artificial aging hardening of 6151 plate

In order to further explore the effect of natural aging on artificial aging hardening, 6151 aluminum alloy was artificially aged at 200 °C for 2 h during 0~14 days of natural aging, and the hardness value curve with natural aging time was obtained. The results are shown in Fig. 5. It can be seen from Fig. 6 that with the increase of natural aging time, the hardness value before artificial aging gradually increases, and tends to be stable with time. The hardness value after artificial aging gradually decreases with the increase of natural aging. After artificial aging treatment, there is a significant improvement on hardness value reached by the aluminum alloy specimen under the context of natural aging. After one day of natural aging, the hardness value of solution-treated samples increased significantly. This is because the supersaturation of solute atoms increases after solution treatment, with many quenching vacancies formed

in the alloy. Due to the quenching vacancies, the solute atoms precipitate rapidly from the aluminum matrix to form plenty of atomic clusters, which hinders the dislocation that occurs during the deformation of the alloy.

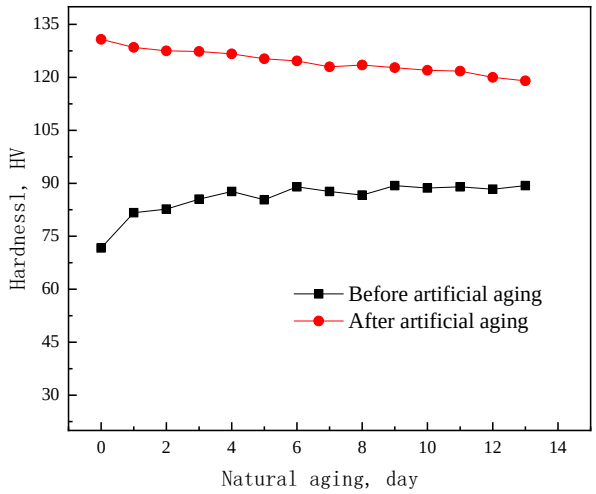

Fig. 6. Effect of natural aging on artificial aging hardening

The strengthening effect of the alloy improved significantly [15]. With the extension of natural aging, the supersaturation of solute atoms diminishes gradually, the precipitation rate of atomic clusters decreases, and the hardness value of the alloy increases slowly and stabilizes [16]. After artificial aging treatment, there is a sharp rise in the hardness value of natural aging specimens. This is attributable to the shift of a large number of GP regions and atomic clusters in the matrix into metastable short rod pre-aging β" phase and acicular β" Phase. Due to the formation of some insoluble atomic clusters during natural aging, β" phase is hindered by these atomic clusters during artificial aging. The amount of β" phase in the alloy is reduced, and the number of phases causes the artificial age hardening effect to diminish gradually with the extension of natural aging time. Besides, the longer the natural aging time, the larger the number of insoluble atomic clusters formed, and the worse the artificial age hardening effect.

4. CONCLUSIONS

1. The artificial age hardening effect of pre-aged aluminum alloy is significantly improved. The higher the pre-aging temperature, the more significant the artificial age hardening effect. At the same artificial aging temperature, the post-aging hardness value increases progressively with the extension of holding time. Given the same artificial aging time, the higher the aging temperature, the more significant the strengthening effect. This is because the supersaturation of solute atoms diminishes gradually, the precipitation rate of atomic clusters decreases, and the hardness value of the alloy increases slowly and stabilizes. The parameters required for the aging process to produce the best artificial aging hardening effect for 6151 aluminum alloy are as follows: a pre-aging temperature of 120 ºC, an artificial aging temperature of 200 ºC and a holding time of 40 minutes.
2. With the extension of artificial aging time, the hardness value of aluminum alloy rises rapidly at first, and then decreases gradually. The response rate of artificial age hardening shows an upward trend with the rise of aging temperature. Since the strengthening effect of the relative matrix is less significant than that of the coherent matrix β" phase, there is a rapid reduction in the hardness of the specimen. After the hardness value peaks, the softening effect becomes more significant at the artificial aging temperature of 200 ºC.
3. The hardness value of aluminum alloy obtained after natural aging treatment is lower than after artificial aging treatment. With the extension of natural aging time, the supersaturation of solute atoms diminishes gradually, the precipitation rate of atomic clusters decreases, and the hardness value of the alloy increases slowly and stabilizes. The effect of artificial aging hardening gradually diminishes. Given an artificial aging temperature of 200 ºC and a holding time of 2 h, the post-aging hardness value gradually decreases with the extension of natural aging, which interferes with the effect of artificial aging.

Acknowledgments

This work was financially supported by Science and Technology planning project of Nanshan Group (Grant No.2022-6-9) and Nanshan University Youth Fund (Grant No.Q202019)

REFERENCES

1. **Jia, Z.H., Ding, L.P., Wu, S.N., Wang, X.L., Liu, Q., Chen, C.Y.** Research Progress on Microstruture and Heat Treatment of 6000 Series Aluminum Alloys Sheet for Automotive Boy *Journal of Materials Engineering* 12 2014: pp. 104 – 113. https://doi: 10.11868/j.issn.1001-4381.2014.12.018
2. **Chen, X., Shu, X., Wang, D., Xu, S., Xiang, W.** Multi-Step Forming Simulation and Quality Control of Aluminum Alloy Automobile Rear Upper Control Arm *Materials* 15 (10) 2022: pp. 3610. https://doi.org/10.3390/ma15103610
3. **Løvik, A.N., Modaresi, R., Müller, D.B.** Long-term Strategies for Increased Recycling of Automotive Aluminum and Its Alloying Elements *Environmental Science & Technology* 48 (8) 2014: pp. 4257 – 4265. https://doi.org/10.1021/es405604g
4. **Zhao, X.Y., Wang, B.X., Li, L., Lian, J.B.** Effect of Deformation and Heat Treatment on Microstructures and Mechanical Properties of 2024 Aluminum Alloy *Nonferrous Metals Engineering* 5 (3) 2015: pp. 1 – 4. https://doi: 10. 3969 /j. issn. 2095 1744.2015.03.001
5. **Tisza, M., Lukács, Z.** High Strength Aluminum Alloys in Car Manufacturing *IOP Conference Series: Materials Science and Engineering* 418 (1) 2018: pp. 012033. https://doi: 10.1088/1757-899X/418/1/012033
6. **Li, Y., Gao, G.J., Wang, Z.D., Di, H.S., Li, J.D., Xu, G.M.** Effects of The Mg/Si Ratio on Microstructure, Mechanical Properties, and Precipitation Behavior of Al–Mg–Si–1.0 wt%-Zn alloys *Materials* 11 (12) 2018: pp. 2591.

https://doi.org/10.3390/ma11122591

7. **Utsunomiya, H., Tada, K., Matsumoto, R., Watanabe, K., Matsuda, K.** Nano Precipitation and Hardening of Die-Quenched 6061 Aluminum Alloy *Journal of Nanoscience and Nanotechnology* 18 (3) 2018: pp. 2200 – 2202. https://doi.org/10.1166/jnn.2018.15007
8. **Wang, C.Y.** Study on Repid Solution and Aging Treatment Process and Mechanism of 6061 Aluminum Alloy Sheets *Harbin Institute of Technology* 2021: pp. 1 – 68. http://doi.org/10.27061/d.cnki.ghgdu.2021.004635.
9. **Aruga, Y., Kozuka, M., Takaki, Y., Sato, T.** Effects of Natural Aging after Pre-aging on Clustering and Bake-hardening Behavior in An Al-Mg-Si Alloy *Scripta Materialia* 116 2016: pp. 82 – 86. http://dx.doi.org/10.101 6/j.scriptamat.2016.01.019
10. **Chen, H.M., Li, K., Yang, M.J., Zhang, Z., Kong, Y., Lu, Q., Du, Y.** Effect of Electron Beam Irradiation in TEM on The Microstructure and Composition of Nanoprecipitates in Al-Mg-Si alloys *Micron* 116 2018: pp. 116 – 123. https://doi.org/10.1016/j.micron.2018.10.003
11. **Shen, C.H., Ou, B.L.** Pre-Ageing to Improve the Microstructure and Tensile Properties of Al-0.72Mg-0.42Si-0.1Cu Artificially Aged Alloy *Canadian Metallurgical Quarterly* 47 (4) 2008: pp. 449 – 458. https://doi.org/10.1179/cmq.2008.47.4.449
12. **Abouarkoub, A., Thompson, G.E., Zhou, X., Hashimoto, T., Scamans, G.** The Influence of Prolonged Natural Aging on the Subsequent Artificial Aging Response of The AA6151 Automotive Alloy *Metallurgical & Materials Transactions A* 46 (9) 2015: pp. 4380 – 4393. https://doi.org/10.1007/s11661-015-3043-9
13. **An, W., Heo, J., Jang, D.C., Euh, K.J., Jung, I.D., Kim, S., Sung, H.** Microstructural Evolution of Al-Zn-Mg-Cu Alloys in Accordance with Homogenization Time *Journal of Nanoscience and Nanotechnology* 20 (11) 2020: pp. 6890 – 6896. https://doi: 10.1166/jnn.2020.18808. PMID: 32604532
14. **Ding, L.P., Weng, Y.Y., Wu, S.N., Sanders, R.E., Jia, Z.H., Liu, Q.** Influence of Interrupted Quenching and Pre-aging on the Bake Hardening of Al-Mg-Si Alloy *Materials Science & Engineering A* 651 (4) 2016: pp. 991 – 998. https://doi.org/10.1016/j.msea.2015.11.050
15. **Cao, L., Rometsch, P.A., Couper, M.J.** Clustering Behaviour in An Al–Mg–Si–Cu Alloy During Natural Ageing and Subsequent Under-ageing *Materials Science & Engineering A* 559 (3) 2013: pp. 257 – 261. https://doi.org/10.1016/j.msea.2012.08.093
16. **He, S.Z., Wang, J., Zhang, D.L., Wu, Q., Kong, Y., Du, Y.** A First-Principles Study of The Cu-Containing β" Precipitates in Al-Mg-Si-Cu Alloy *Materials* 14 (24) 2021: pp. 7879. https://doi.org/10.3390/ma14247879